

Finite element analysis on concrete-encased CFST columns subjected to heating and cooling fire

*Shu-Lan Hou¹⁾, Lin-Hai Han²⁾ and Tian-Yi Song³⁾

^{1), 2)} *Department of Civil Engineering, Tsinghua University, Beijing 100084, PR China*

³⁾ *Institute for Infrastructure Engineering, University of Western Sydney, Penrith NSW
2751, Australia*

¹⁾ hsl11@mails.tsinghua.edu.cn

ABSTRACT

This paper develops a finite element analysis (FEA) model to simulate the behavior of concrete-encased CFST columns under combined axial load and fire including heating and cooling phases. Experimental data, including concrete-encased CFST column tests at ambient temperature, CFST column and RC column tests in fire and CFST column tests after fire, are used to validate the established FEA model, and generally the accuracy of predicted results is acceptable. Based on the FEA model, the temperature distribution, failure mode and deformation of the concrete-encased CFST column in heating and cooling phases are investigated. Finally, a parametric study is conducted to investigate the influence of various parameters on the performance of concrete-encased CFST columns failed in cooling fire.

Keywords: Concrete-encased CFST column; Finite element analysis; Heating and cooling fire; Parametric analysis; Failure mode

1. INTRODUCTION

Concrete-encased CFST column is a type of composite column which is made up of internal concrete filled steel tube (CFST) and outer layer reinforced concrete. This type of composite column has been widely used in high-rise buildings due to its superior structural performance (Lin and Li 2008). Fig. 1 shows a concrete-encased CFST column under construction (Huang et al. 2008), in which, the typical square cross-section with circular internal CFST is adopted.

Recently, the building fire safety has been paid more attentions due to the increased fire disasters. For a real building subjected to fire, the structure or members usually experience a combined loading and fire phase (Song et al. 2010), including ambient

¹⁾ Graduate Student

²⁾ Professor

³⁾ Doctor

loading phase, heating phase with constant external load and cooling phase with constant external load. If the structure survives from the fire, the post-fire performance of the structure can be evaluated by increasing the loads, which is named as the post-fire loading phase. The significant influence of the cooling phase of the fire and initial load on the behavior of structures in and after fire has been identified by the researches on CFST columns (Han 2007; Yang et al. 2008). However, no corresponding research has been done on the concrete-encased CFST columns.

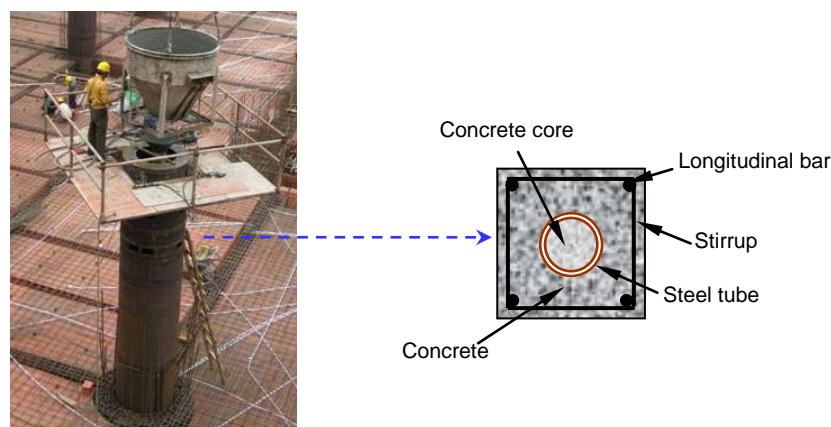


Fig. 1 A concrete-encased CFST column under construction (Huang et al. 2008)

Previous studies mainly focus on the behavior of concrete-encased CFST column in heating fire phase or post-fire phase without initial load. Feng et al. (2008) theoretically and experimentally analyzed the temperature distribution and the post-fire residual load bearing capacity of the concrete-encased CFST column; Liu (2007) conducted a finite element analysis to investigate the ultimate bearing capacity of concrete-encased CFST column subjected to ISO-834 standard heating fire.

Therefore, in this paper, in order to investigate the fire behavior of concrete-encased CFST column exposed to heating and cooling fire, and the post-fire behavior after exposed to heating and cooling fire with initial load, a finite element analysis (FEA) model of concrete-encased CFST column is tentatively established. Based on the FEA model, the behavior of concrete-encased CFST column subjected to combined loading and fire phase is analyzed, and a parametric study is conducted to investigate the behavior of concrete-encased CFST columns failed in the cooling phase.

2. ESTABLISHMENT OF FINITE ELEMENT ANALYSIS MODEL

Sequentially-coupled thermal-mechanical analysis method provided in ABAQUS software is adopted to build a numerical model to capture the response of concrete-encased CFST column in the ambient loading, heating, cooling and post-fire loading phases. The simulation includes two parts, which are thermal analysis model and mechanical analysis model. The details are introduced below.

2.1 Thermal analysis model

Yang et al. (2008), Song et al. (2010) and Tan (2012) established FEA models to simulate the temperature distributions of CFST columns and SRC columns under ISO-834 (1980) heating and cooling fire, and the simulated results are validated by comparing with the tested results. Therefore, for the concrete-encased CFST column in heating and cooling fire, the same thermal analysis modeling method was adopted. For the thermal properties of steel and concrete, the thermal conductivity, density and specific heat formulas reported by Lie (1994) were used in heating and cooling phases.

In heating phase, the heat transfers from the environment to the column surface through heat convection and radiation, and then the heat transfers from column surface to the environment when the temperature of column is higher than the environment in the cooling phase. The heat convective coefficient of $25 \text{ W}/(\text{m}^2\text{K})$ and the resultant heat emissivity of 0.5 were adopted according to ECCS (1988). For the interface between steel and concrete, the constraint type "Tie" was adopted to simulate a fully heat transfer. Fig. 2 illustrates the boundary conditions and element divisions of the established thermal analysis model. The rigid endplate and concrete adopted 8-node linear heat transfer brick elements (DC3D8), the steel tube was modeled using 4-node heat transfer quadrilateral shell elements (DS4), and the longitudinal bar and stirrup utilized 2-node heat transfer link elements (DC1D2).

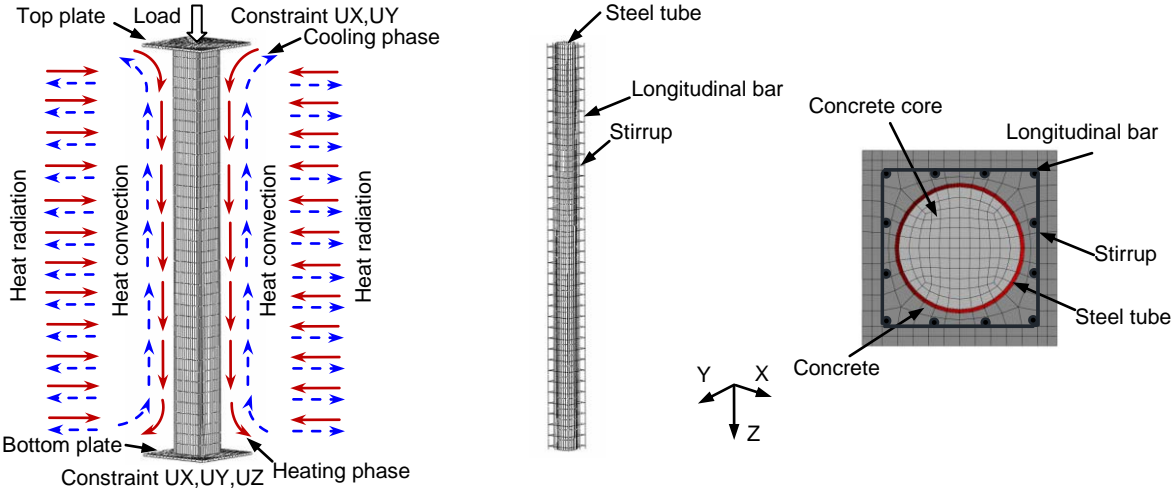


Fig. 2 Meshing and boundary conditions of the FEA model

2.2 Mechanical analysis model

From the thermal analysis model, the temperature corresponding to each node in the model was calculated, and then the temperature results were input into the mechanical analysis model to simulate fire condition. To capture the mechanical behavior of concrete-encased CFST column in the ambient loading, heating, cooling and post-fire loading phases, the mechanical properties of steel and concrete in ambient, heating, cooling and post-fire phases must be decided accordingly.

For the concrete-encased CFST column, the material mechanical properties, including steel property, core concrete property confined by the steel tube and concrete property outside the steel tube, were decided based on the previous research. Song et al. (2010) simulated the behavior of CFST stub columns under combined load and fire,

and the mechanical property formulas of steel and confined core concrete in ambient, heating, cooling and post-fire phases were proposed. Here, the same formulas were adopted to the concrete-encased CFST column model. For the concrete outside the steel tube, the material property model suggested by Tan (2012) was adopted, which has been used to simulate the behavior of SRC columns subjected to the heating and cooling fire successfully. The details for the material properties of steel and concrete can be found in Song et al. (2010) and Tan (2012).

The research outcome reported by Guo and Shi (2003) indicates that concrete thermal creep strain and concrete instantaneous thermal strain induced by high temperature have an important influence on the structural deformations in fire. Tan (2012) built FEA models on steel reinforced concrete columns and frames after fire, in which the concrete thermal creep strain and concrete instantaneous thermal strain models provided by Anderberg and Thelandersson (1976) were employed to consider their influence by using user subroutines in ABAQUS software, and reasonable results were obtained. Therefore, in this paper, the same models and modeling methods were adopted to consider the influence of concrete thermal creep strain and instantaneous thermal strain in the heating and cooling phases.

Fig. 2 shows the meshing and boundary conditions of the mechanical analysis model. 8-node linear brick elements with reduced integration and hourglass control (C3D8R) were used for the rigid endplate and concrete, 4-node shell elements with reduced integration, hourglass control and finite membrane strains (S4R) were used for the steel tube, and 2-node linear 3-D truss elements (T3D2) were used to model the steel bars. Pin-pin end was applied on the top and bottom endplates of the composite column. The interaction between the steel tube and concrete was simulated by a contact pressure model in the normal direction and a Coulomb friction model in the tangential direction. The Coulomb coefficient of friction was taken as 0.6 according to Han (2007). The "Tie" or "Embedded" was chosen as the constraint of the steel bars and outer concrete.

3. VERIFICATIONS ON THE FEA MODEL

Due to the lack of the experiments on concrete-encased CFST columns under the heating and cooling fire, the FEA model is validated indirectly by comparing with the test data of axially loaded concrete-encased CFST columns at ambient temperature, CFST columns and RC columns in fire and CFST columns after fire.

3.1 Tests on concrete-encased CFST column at ambient temperature

Kang and Qian (2006), Chen (2002), Nie et al. (2005) and Li (2005) reported test data on concrete-encased CFST stub columns under axial and eccentric compression. These test results are used to validate the FEA model. Fig. 3 shows some of the comparisons between tested and predicted load (N) versus longitudinal strain (ϵ) curves, where B is the outside dimension of square column, D and t are the outside diameter and thickness of circular steel tube, f_y is the steel yield strength, $f_{cu,i}$ and $f_{cu,o}$ are the concrete cube strength inside and outside steel tube respectively. Fig. 4 shows the comparisons between tested and predicted ultimate bearing capacities. It can be seen that the predicted results are acceptable.

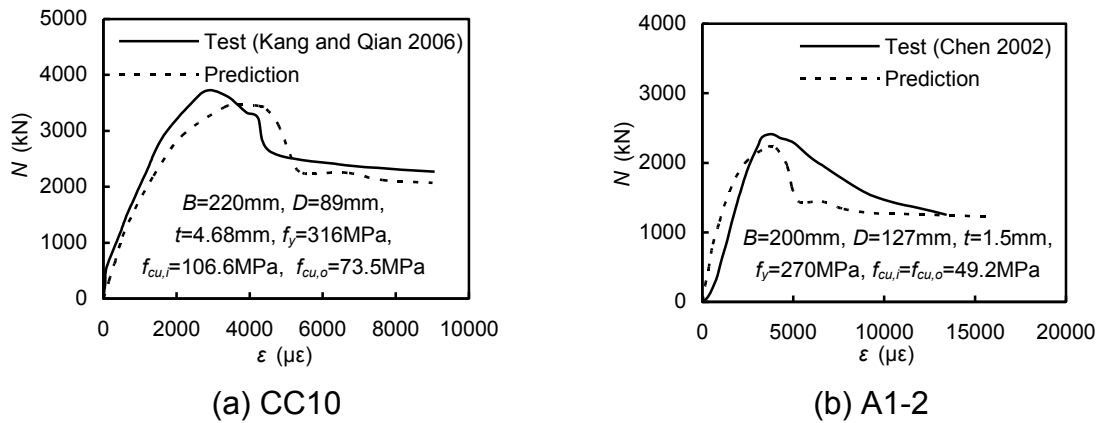


Fig. 3 Comparison between tested and predicted N - ε curves

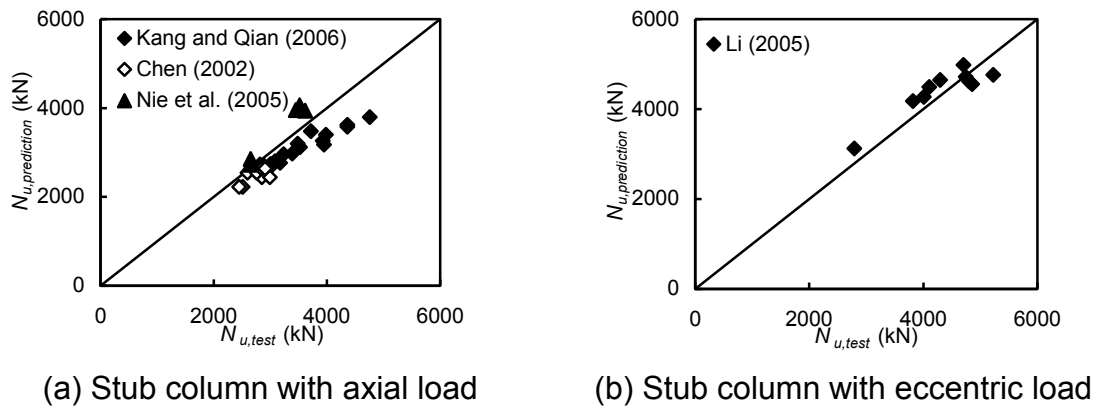


Fig. 4 Comparison between tested and predicted ultimate bearing capacities

3.2 Tests on CFST column and RC column in fire

Fire resistance test data of CFST columns and RC columns are used to validate the FEA model. Fig. 5 shows some of the comparisons between tested and predicted column axial displacement (Δ) versus time (t) curves, where e is the axial load eccentricity, N_F is the initial load applied on the column. The tested result on CFST column in Fig. 5(a) is from Han (2007), and the tested result on RC columns in Fig. 5(b) is from Lie et al. (1984). It can be found that the calculated fire resistance of RC columns is higher than the experimental value, this may be attributed to the fact that concrete spalling occurs at the maximum lateral deformation of the column, and this influence cannot be considered in the proposed FEA model. In general, the accuracy of the calculated results is acceptable.

3.3 Tests on CFST column after exposed to ISO-834 standard fire

Han (2007) carried out four tests on concrete filled circular hollow section (CHS) columns after exposed to ISO-834 standard fire. Table 1 describes the information of testing members and residual load bearing capacities of columns, in which, L is the overall length of columns, λ is the column slenderness ratio ($\lambda=4L/D$), t_h is the heating

time, N_{ue} and N_{uc} are the experimental and calculated residual load bearing capacities of specimens, respectively. It can be found that the calculated residual load bearing capacities are close to the tested results, and generally conservative results can be obtained. Fig. 6 shows some of the comparisons between tested and predicted load (N) versus mid-height deflection (u_m) curves. It can be found that the tested and predicted results are in good agreement.

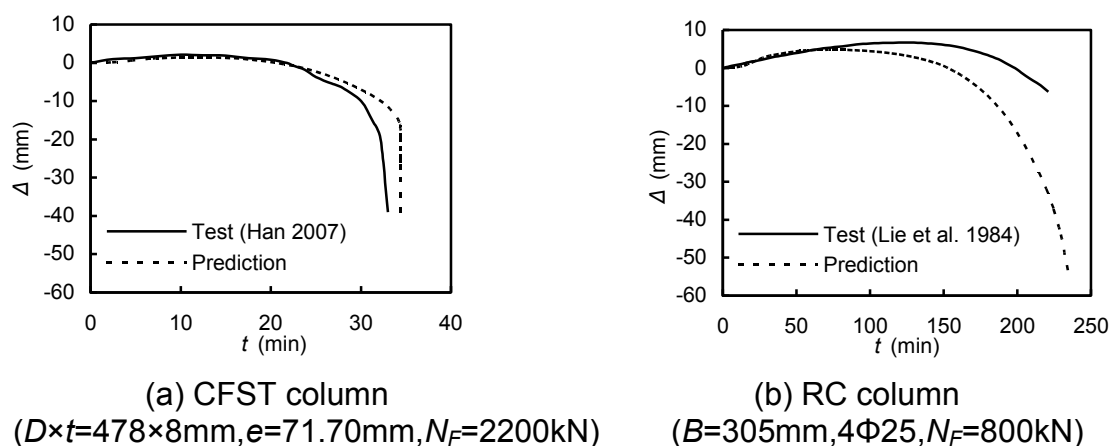


Fig. 5 Comparison between tested and predicted Δ - t curves of CFST and RC columns

Table 1 Specimen details and residual ultimate strength of CFST column

Label	Specimen size $D \times t \times L$ (mm)	λ	e (mm)	f_y (MPa)	f_{cu} (MPa)	t_h (min)	N_{ue} (kN)	N_{uc} (kN)	$\frac{N_{uc}}{N_{ue}}$
C1	108×4.32×600	22.2	0	355.7	71.3	90	632.1	516.0	0.816
C2	108×4.32×600	22.2	15	355.7	71.3	90	387.1	315.7	0.816
C3	108×4.32×1200	44.4	0	355.7	71.3	90	362.2	339.7	0.938
C4	108×4.32×1200	44.4	15	355.7	71.3	90	227.4	248.3	1.092

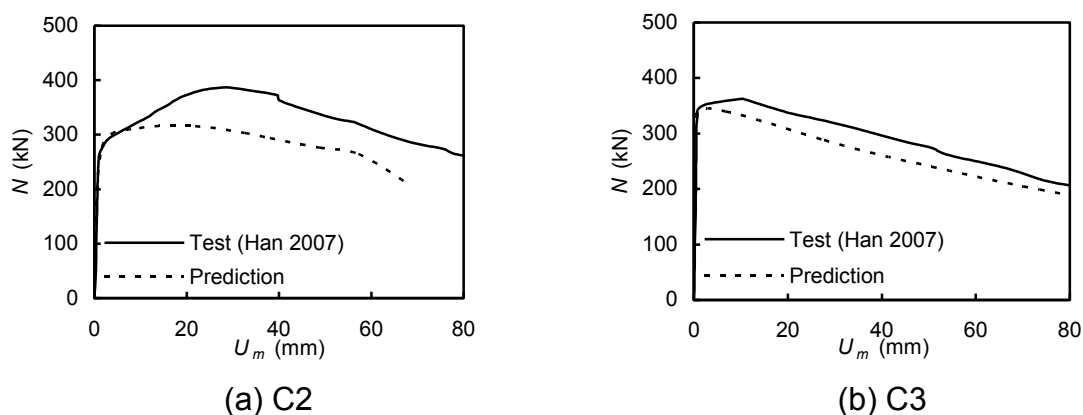


Fig. 6 Comparison between tested and predicted N - u_m curves of CFST columns

Based on the verified FEA model, the behavior of concrete-encased CFST columns subjected to heating and cooling fire is studied.

4. ANALYSIS ON THE BEHAVIOR OF CONCRETE-ENCASED CFST COLUMNS

According to the Technical specification for steel tube-reinforced concrete column structure (CECS 188:2005), the basic calculation conditions of concrete-encased CFST column are: $B=300\text{mm}$, $D\times t\times L=200\times 6\times 3800\text{mm}$, heating time ratio $t_0=0.8$ ($t_0=t_h/t_R$, where t_R is the fire resistance), load ratio $n=0.5$ ($n=N_F/N_u$, where N_u is the ultimate strength at ambient temperature), CFST ratio $\alpha_{cfst}=0.35$ ($\alpha_{cfst}=A_{cfst}/A_0$, where A_{cfst} is the cross sectional area of concrete filled steel tube in it, A_0 is the cross sectional area of total cross-section), reinforcement ratio $\rho_s=4.12\%$ ($\rho_s=A_{ss}/A_{co}$, where A_{ss} is the total cross sectional area of longitudinal reinforcements, A_{co} is the cross sectional area of outer layer concrete), steel yield strength $f_y=345\text{ MPa}$.

4.1 Temperature versus time curves

Fig. 7 shows the temperature versus time curves of sectional characteristic points in the heating and cooling phases ($t_h=44\text{min}$). When the outer surface of the column section starts cooling, the interior temperatures still keep increasing gradually and then reach their peak temperatures in cooling phase. Using location 3 as an example, its temperature is 142°C at the end of heating phase, but its maximum temperature of 306°C occurs at 80 minutes after the end of heating phase. There is a distinct trend of maximum temperature reduction from the outer to the inner of the column section. The maximum temperature of reinforcing bar at location 5 is higher than location 4, and the peak temperature of steel tube is much lower than the rebar owing to the protection of outer layer reinforced concrete. The temperatures of internal and external steel tube surfaces are approximately the same due to the excellent thermal conductivity property of steel.

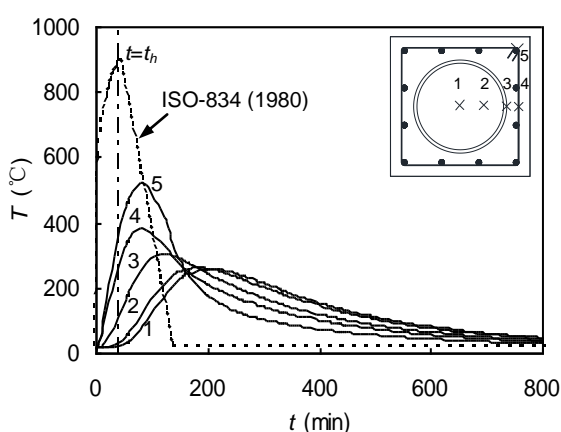


Fig. 7 Temperature (T) versus time (t) curves

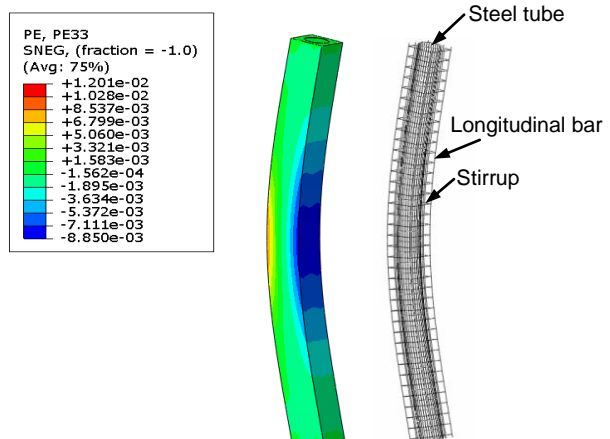


Fig. 8 Failure mode

In Fig. 7, it can be found that the peak temperatures of location 1 and location 2 are very close. Besides, the temperature versus time relation curves turn to a relatively plateau stage when the temperatures of location 1 and location 2 are close to 100°C. This is because the evaporation of moisture in concrete will absorb significant amounts of heat and slow down the rate of heating. This phenomenon is much more obvious at locations away from the outside surface of column since water evaporation is slower and the effect of absorbing heat is more distinctive in the inner of the column section.

4.2 Failure mode

Fig. 8 shows the failure mode of the concrete-encased CFST column during the cooling phase, where PE represents the longitudinal plastic strain of concrete. It can be seen that the maximum concrete compressive plastic strain occurs at the middle height of column, and the column fails due to the overall buckling induced by the degraded concrete properties. Besides, the failure mode of the inner steel tube and steel bars indicates that no local buckling occurs in steel tube and bars due to the protective effect of outer concrete.

4.3 Axial deformation

Fig. 9 shows the typical axial displacement versus time curves of concrete-encased CFST columns during the entire stage of fire exposure, the curves can be divided into three phases: heating phase (I), cooling phase (II) and failure phase (III).

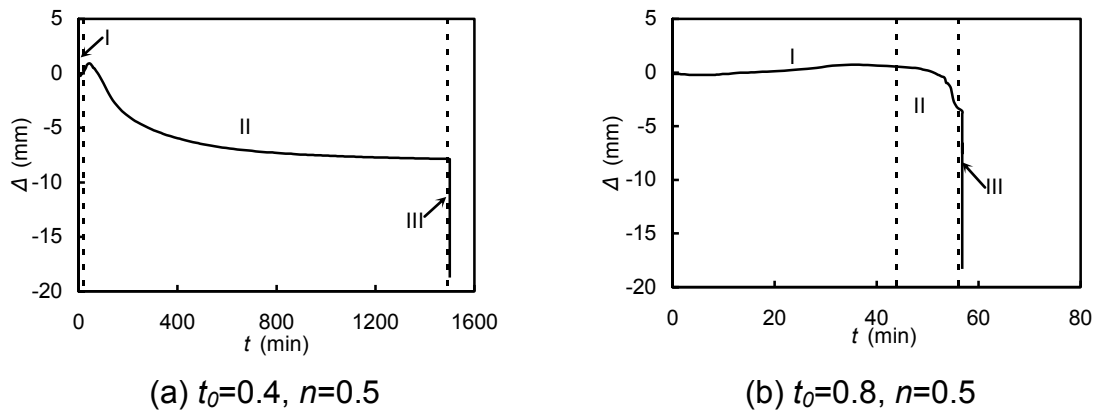


Fig. 9 Δ - t curves of concrete-encased CFST columns

In heating phase, the extension deformation induced by thermal expansion is larger than the contraction deformation induced by the deteriorations of materials since the temperatures of most regions of the column are still lower, hence, there is an extension of column during this phase. In cooling phase, the stiffness of column is greatly weakened as the temperature raising, the contraction deformation of column is increasing gradually. Finally the column fails when the rate of reduction in column axial deformation increases rapidly. For the same column, if the heating time ratio t_0 is big enough, the temperatures in the interior parts become much higher in the cooling

phase than the column with a smaller heating time ratio, and the degradation of the material strength is more serious in the cooling phase, which may induce the column failure during the cooling phase as shown in Fig. 9(b). Otherwise, if the column survives from the heating and cooling fire, and then increase the applied load, the column will fail in the post-fire stage as shown in Fig. 9(a).

5. PARAMETRIC ANALYSIS

Parameters that may affect the behavior of concrete-encased CFST column in cooling phase include sectional dimension, slenderness ratio, CFST ratio, heating time ratio, load ratio, load eccentricity ratio, reinforcement ratio, stirrup spacing, steel yield strength and concrete cube strength. Here, this research will focus on investigating the influence of some important parameters, which are the heating time ratio (t_0), load ratio (n), CFST ratio (α_{cfst}), reinforcement ratio (ρ_s) and steel yield strength (f_y).

The composite column may fail at heating, cooling or post-fire loading phases corresponding to different calculation conditions. Here, the research will focus on investigating the case that the composite column fails in the cooling phase. Therefore, in order to realize the case, the heating time ratio (t_0), which affects the failure case of the composite column directly, is set greater than 0.6 for all the calculating conditions.

Fig. 10 shows the predicted axial deformation (Δ) versus time (t) curves corresponding to various parameters, including heating time ratio $t_0=0.6\sim 0.9$, load ratio $n=0.3\sim 0.7$, CFST ratio $\alpha_{cfst}=0.22\sim 0.35$, reinforcement ratio $\rho_s=3.15\%\sim 5.21\%$, steel yield strength $f_y=235\sim 420$ MPa. It can be seen that:

(1) The influences of heating time ratio, load ratio and CFST ratio on the Δ - t curves of concrete-encased CFST columns, as shown in Figs. 10 (a)-(c), are significant. As the increasing of heating time ratio and load ratio, the time that columns reach ultimate stage in the cooling phase decreases. The opposite tendency can be found for the CFST ratio.

(2) For the reinforcement ratio in Fig. 10(d), the predicted results indicate that its influence is minor. It's attributed to the fact that the contribution of steel bars to the load bearing capacity of the composite column is minor compared with the other parts, such as steel tube and concrete.

(3) The steel yield strength has moderate effect on the development of the axial deformation of columns during the heating and cooling phases. When the steel yield strength is less than 345 MPa, the time that columns reach ultimate stage in the cooling phase increases as the increasing of steel yield strength, but the influence is minor when the steel yield strength exceeds 345 MPa.

6. CONCLUSIONS

Based on the limited research in this paper, the following conclusions can be drawn:

(1) A FEA model was established to simulate the behavior of concrete-encased CFST column in heating and cooling fire. The accuracy of the FEA model was verified against the existing test data.

(2) The interior parts of the column reach the maximum temperatures in the cooling phase of fire, which may induce the composite columns' failure due to the degradation

of material properties in this phase.

(3) The influences of heating time ratio, load ratio, CFST ratio, reinforcement ratio and steel yield strength on the behavior of concrete-encased CFST column in cooling phase were investigated. It is found that the influences of heating time ratio, load ratio and CFST ratio are significant.

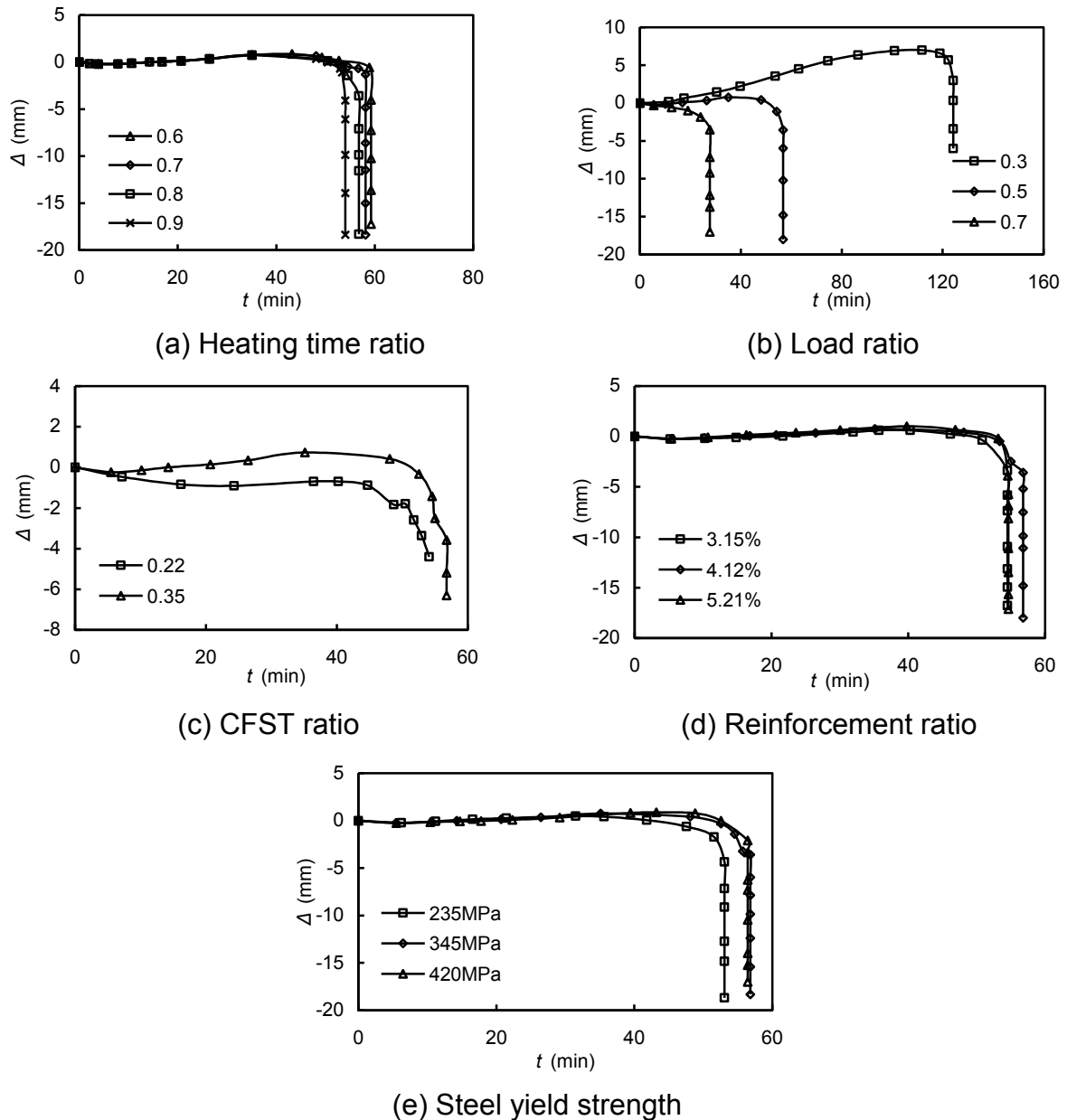


Fig. 10 Influence of parameters on the Δ - t curves of concrete-encased CFST columns

7. ACKNOWLEDGEMENTS

The research reported in the paper is part of "The 12th-Five-Year Plan" National

Key Technologies R&D Program (2012BAJ07B01) of China. The financial support is highly appreciated.

REFERENCES

- Anderberg, G.Y. and Thelandersson, S. (1976), "Stress and deformation of concrete at high temperatures: 2 experimental investigation and material behaviour", *Bulletin 54, Lund Institute of Technology*, Lund.
- Chen, Z.Y. (2002), "Study of the method for design and calculation of HSC columns reinforced with concrete filled steel tube." PhD Dissertations, Dalian University of Technology, Dalian, China [in Chinese].
- CECS 188:2005. (2005), "Technical specification for steel tube-reinforced concrete column structure." Standardization institute of Chinese construction note [in Chinese].
- ECCS-Technical Committee 3. (1988), "Calculation of the fire resistance of centrally loaded composite steel-concrete columns exposed to the standard fire." Fire safety of steel structures-technical note.
- Feng, Y.H., Shen, Tao, Lou, W.J. and Zhou, Jun. (2008), "The study of residual load bearing capacity of column reinforced by inner circular steel tube after fire." *Indus. Constr.*, Vol. 38(3), 16-19 [in Chinese].
- Guo, Z.H. and Shi, X.D. (2003), *Behaviour of Reinforced Concrete at Elevated Temperature and Its Calculation*, Tsinghua University Press, Beijing, China [in Chinese].
- Huang, Y.J., Yao, G.H., Song, B.D. and Peng, Z.C. (2008), "Application of concrete filled steel tubular column in the tower of Zhuoyue•Huanggang century center in Shenzhen city." *Guangzhou Architecture Civil Engineering*, Vol. 7(7), 3-5 [in Chinese].
- Han, L.H. (2007), *Concrete Filled Steel Tubes Structure-Theory and Practice*, Science Press, Beijing, China [in Chinese].
- ISO-834. (1980), "Fire-resistance tests-elements of building construction." International Standard, ISO834: Amendment 1, Amendment 2 .
- Kang, H.Z. and Qian, J.R. (2006), "An experiment study of axial compressive strength of concrete filled steel tube composite columns." *Build. Struct.S1*, Vol. 36(9), 22-25 [in Chinese].
- Lin, L.Y. and Li, Q.G. (2008), "Design concept and analysis of technical economy for steel tube reinforced concrete column." *Build. Struct.*, Vol. 38(3), 17-21[in Chinese].
- Liu, D.P. (2007), "Nonlinear analysis of axially compressed concrete steel tube composite columns filled (CFST) under fire." Master Dissertations, Chang'an University, Xi'an, China [in Chinese].
- Lie, T.T. (1994), "Fire resistance of circular steel columns filled with bar-reinforced concrete." *J. Struct. Eng., ASCE*, Vol. 120(5), 1489-1509.
- Li, Peng. (2005), "Experimental and theoretic study on compression characteristics of composite column with core of high-strength concrete filled steel tube." Master Dissertations, Zhejiang University, Zhejiang, China [in Chinese].
- Lie, T.T., Lin, T.D., Allen, D.E. and Abrams, M.S. (1984), "Fire resistance of reinforced concrete columns." Division of Building Research, DBR Report, No.1167, National Research Council of Canada, Ottawa.

- Nie, J.G., Zhao, Jie and Bai, Yu. (2005), "Bearing capacity of axially compressed core columns having concrete-filled steel tubes." *Journal of Tsinghua University (Science and Technology)*, Vol. 45(9), 1153-1156 [in Chinese].
- Song, T.Y., Han, L.H. and Yu, H.X. (2010), "Concrete filled steel tube stub columns under combined temperature and loading." *J. Constr. Steel. Res.*, Vol. 66(3), 369-384.
- Tan, Q.H. (2012), "Performance of steel reinforced concrete (SRC) column and portal frame after exposure to fire." PhD Dissertations, Tsinghua University, Beijing, China [in Chinese].
- Yang, Hua, Han, L.H. and Wang, Y.C. (2008), "Effects of heating and loading histories on post-fire cooling behavior of concrete-filled steel tubular columns." *J. Constr. Steel. Res.*, Vol. 64(5), 556-570.